

Long-range cooperative binding of kinesin to a microtubule in the presence of ATP

Etsuko Muto,^{1,2} Hiroyuki Sakai,³ and Kuniyoshi Kaseda⁴

¹Form and Function Group, PRESTO, JST, Mino, Osaka 562-0035, Japan

²Brain Developmental Research Group, RIKEN Brain Science Institute, Saitama 351-0198, Japan

³Laboratory for Neuroinformatics, Advanced Technology Development Group, RIKEN Brain Science Institute, Saitama 351-0198, Japan

⁴Gene Function Research Center, National Institute of Advanced Industrial Science and Technology, Ibaraki 305-8562, Japan

Interaction of kinesin-coated latex beads with a single microtubule (MT) was directly observed by fluorescence microscopy. In the presence of ATP, binding of a kinesin bead to the MT facilitated the subsequent binding of other kinesin beads to an adjacent region on the MT that extended for micrometers in length. This cooperative binding was not observed in the presence of ADP or 5'-adenylylimidodiphosphate (AMP-PNP), where binding along the MT was random. Cooperative binding also was induced by an

engineered, heterodimeric kinesin, WT/E236A, that could hydrolyze ATP, yet remained fixed on the MT in the presence of ATP. Relative to the stationary WT/E236A kinesin on a MT, wild-type kinesin bound preferentially in close proximity, but was biased to the plus-end direction. These results suggest that kinesin binding and ATP hydrolysis may cause a long-range state transition in the MT, increasing its affinity for kinesin toward its plus end. Thus, our study highlights the active involvement of MTs in kinesin motility.

Introduction

Kinesin is a molecular motor that transports organelles along a microtubule (MT) using the energy of ATP hydrolysis. Conventional kinesin is highly processive and can move across hundreds of tubulin dimers ($>1 \mu\text{m}$) without dissociating from the MT (Howard et al., 1989; Block et al., 1990). This processive movement has been explained by a “hand-over-hand” model in which the two heads of a kinesin alternately interact with the MT (Schnapp et al., 1990; Hackney, 1994; Howard, 1996). A nucleotide-dependent conformational change in the “neck-linker”, a small peptide emerging from the COOH terminus of the catalytic core, is considered crucial for the “walking” mechanism of two-headed kinesin (Rice et al., 1999). The model attributes the movement to structural change in the kinesin, whereas MTs are regarded as merely a passive track.

On the other hand, in actomyosin, the motor system in muscle, several reports have indicated that the structure and dynamics of actin filaments may play an active role in motility. When actin filaments interact with heavy meromyosin in the presence of ATP, a rapid and significant bending motion or

accelerated diffusion of actin filaments was observed, indicating that some kind of conformational change may be occurring in actin filaments (Yanagida et al., 1984; Burlacu and Borejdo, 1992). Moreover, an experiment using intrastrand cross-linked actin demonstrated that the velocity of actin filaments in an *in vitro* motility assay was reduced with an increase in actin cross-linking, whereas the rigor myosin subfragment (S1) binding to actin filaments and the acto-S1 ATPase activity were virtually unaffected by the cross-link (Kim et al., 1998). This indicated that the dynamic property of actin filaments that is essential for motility might be inactivated by the intrastrand cross-link. These results in the actomyosin system raise the possibility that in the corresponding MT–kinesin system, MTs are more than simply a passive track.

To study the dynamic properties of MTs during motility, we directly observed the binding and motility of kinesin-coated beads along a single MT. We find that in the presence of ATP, a kinesin-coated bead binds to a MT in a cooperative manner with a large cooperative range, in the order of micrometers in length. The result suggests that the MT has both high and low affinity states for kinesin, and binding of kinesin induces the high affinity state over an extended range. In contrast to this cooperative binding in the presence of ATP, in the presence of ADP or 5'-adenylylimidodiphosphate (AMP-PNP), binding was random along the MT, indicating that this state transition is closely related to motility.

Correspondence to Etsuko Muto: emuto@brain.riken.go.jp

K. Kaseda's present address is Molecular Motor Group, Marie Curie Research Institute, Surrey, RH8 0TL, UK.

Abbreviations used in this paper: AMP-PNP, 5'-adenylylimidodiphosphate; MT, microtubule; PDD, probability density distribution.

The online version of this article contains supplemental material.

Results and discussion

To observe kinesin–MT interactions, native kinesin purified from bovine brain was first coated onto the surface of fluorescent latex beads (0.2 μm in diameter) at a molar ratio of 17 to 1. These kinesin-coated beads were then combined with rhodamine-labeled MTs in the presence of ATP, and their binding to a MT was directly observed by conventional fluorescence microscopy. In this experimental condition, the kinesin beads bound to the MT at an average binding frequency of 0.018 $\mu\text{m}^{-1} \text{s}^{-1}$ and moved toward the MT plus end at a velocity of $0.90 \pm 0.15 \mu\text{m/s}$ (mean \pm SD). Due to the high density of bound kinesin, most of the beads that had bound to the MT ($97 \pm 4\%$) did not dissociate from the MT until reaching the plus end (Block et al., 1990).

Fig. 1 A shows sequential images of kinesin beads moving on a single MT, taken at 1-s intervals. New bindings are represented by red dots with their color turning yellow in subsequent images. Quite unexpectedly, the binding of kinesin beads was

not completely random, but occurred preferentially in the vicinity of beads that were already moving along the MT. Consequently, a cluster of kinesin beads was formed over several micrometers of MT filament, and longer observation times revealed new clusters being repeatedly formed (Video 1, available at <http://www.jcb.org/cgi/content/full/jcb.200409035/DC1>).

To test the statistical validity of the observed preferential binding, the binding frequency of kinesin beads was calculated as a function of the distance from a moving bead. First, the positions of the beads interacting with a single MT were determined using the image analysis software, NIH image, at 0.33-s intervals (at a rate of 3 frame/s) over an observation period of 8–15 min, which corresponded to between 159 and 205 new binding events. Based on the instantaneous position of each preexisting, moving kinesin bead, a 1- μm window was shifted along the MT in both the plus- and minus-end directions (Fig. 1 B, colored rectangles), and for each

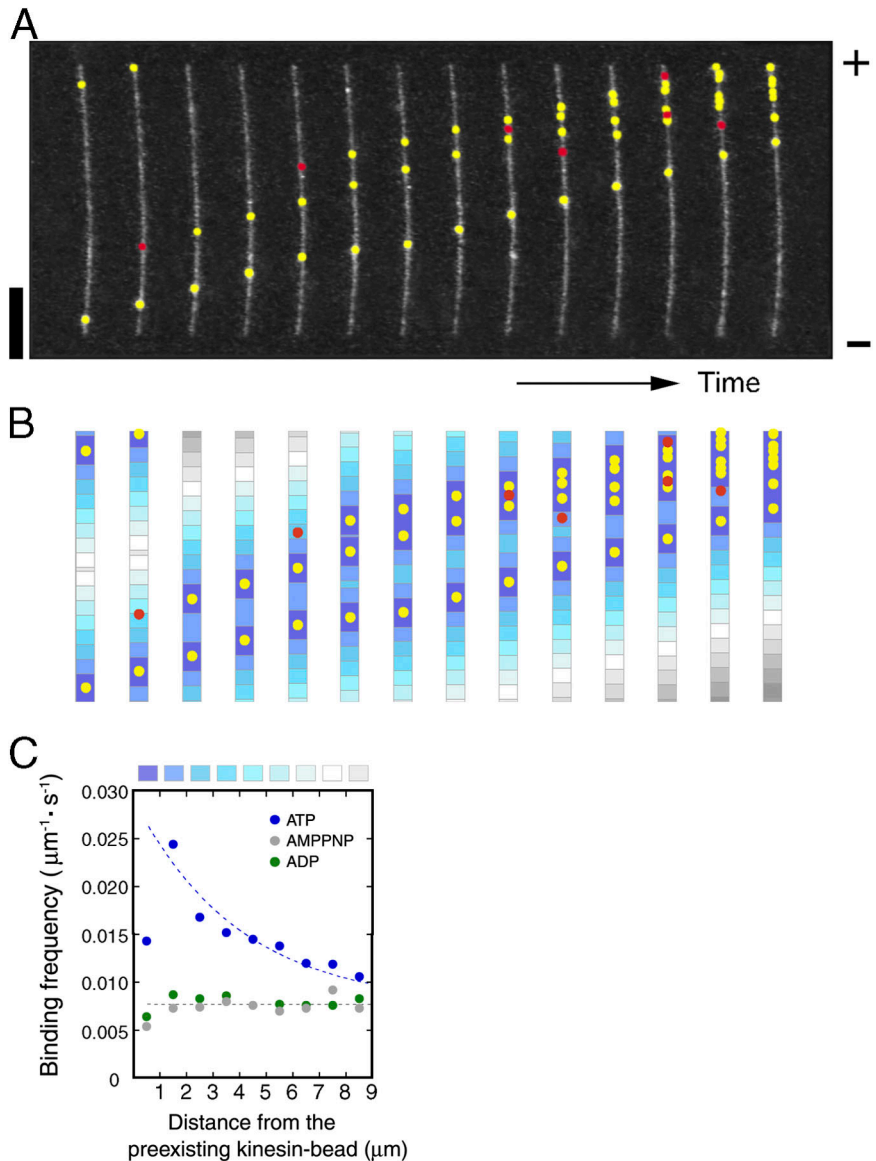


Figure 1. Interaction of kinesin-coated beads with a MT in various nucleotide conditions. (A) Sequential images of kinesin beads interacting with a MT in the presence of 1 mM ATP, taken at 1-s intervals. Bar, 5 μm . (Video 1). (B) Diagrams illustrating how the windows (represented by rectangles of various colors) were defined for the statistical analysis of the binding frequency. The example is taken from the images shown in A. Starting from the position of the preexisting kinesin beads (yellow dots), a window of 1 μm was shifted along a MT in both plus- and minus-end directions until the entire length of MT was covered. (C) The binding frequency calculated as a function of distance from the preexisting kinesin beads. Binding was measured in the presence of 1 mM ATP (blue dot), AMP-PNP (gray dot), and ADP (green dot) at a kinesin-bead concentration of 90 μM . Total number of binding events, number of MTs, and total observation time were 934 binding events, 5 MTs (length = 12.90–18.55 μm), 61 min for ATP; 734 binding events, 65 MTs (length = 11.94–18.10 μm), 114 min for ADP; and 669 binding events, 72 MTs (length = 12.18–18.87 μm) and 115 min for AMP-PNP, respectively. When the position of the kinesin bead was recorded at a higher temporal resolution (10 frame/s), the binding frequency was not affected, indicating that the temporal resolution of 3 frames/s is adequate.

window with a distinct color, the total number of new binding events, N , and the total length of MT, L , was measured. N and L were thus measured in five randomly selected MTs and the results were combined. Finally, the frequency of new binding events in each window was obtained by dividing the combined N by the product of combined L and t ($=N/(L*t)$), where t is the observation time (0.33 s).

Fig. 1 C is a result of such a calculation, showing that binding was actually enhanced in the vicinity of preexisting kinesin beads except for the area immediately surrounding the preexisting kinesin bead. In that area (within 1 μm distance), the binding was slightly suppressed due to physical obstruction of the binding site by the preexisting bead. Statistical significance of the preferential binding was confirmed by the Kolmogorov-Smirnov test of probability density distributions (PDDs; Fig. S1, available at <http://www.jcb.org/cgi/content/full/jcb.200409035/DC1>). This calculation of binding frequency does not depend on any statistical assumptions, because it simply divides the MT into zones depending on the distance from the moving kinesin beads, and calculates the binding frequency in each zone.

Importantly, this cooperative binding was observed only in the presence of ATP. Binding was less frequent and random along the MT in the presence of both ADP and AMP-PNP (Fig. 1 C). It should be noted that the kinesin concentration used here (1.5 nM) was significantly lower than that used previously (6–10 μM) to examine the cooperative binding of kinesin dimers in the presence of AMP-PNP (Vilfan et al., 2001). The cooperative binding observed in the previous study was most likely a result of attractive interaction between kinesin molecules.

Although the binding frequencies were similar for ADP and AMP-PNP, the behavior of the kinesin beads after the binding event was different, reflecting the weak and strong binding states in ADP and AMP-PNP conditions, respectively (Crevel et al., 1996). In the presence of ADP, the position of the kinesin beads changed slightly with time along the MT (diffusion coefficient = 380 nm^2/s), and in some rare occasions, they even dissociated from the MTs ($k_{\text{off}} = 0.004/\text{s}$). In contrast, in the presence of AMP-PNP, the kinesin beads neither

changed their position (diffusion coefficient $\leq 26 \text{ nm}^2/\text{s}$) nor dissociated from the MT once bound.

We next wished to determine if there is any bias in the direction of cooperative binding. In the analysis of binding frequency described above, directionality was not explicitly considered because in situations where multiple beads were simultaneously moving along a MT, it was difficult to determine whether it was the forward or the rear bead that facilitated the new binding. To simplify the analysis, directionality was examined only in cases where a single kinesin bead was moving on the MT before the analysis (Fig. 2 A). The distribution of subsequent new binding events relative to the position of the moving beads was then examined. To guarantee equal opportunity for new binding in either direction, new bindings were included in the statistics only when the available area of MT exceeded 6 μm in length on both sides of the moving kinesin beads. Although such a “lone” situation was relatively rare, records obtained over a total observation period of ~ 4 h (corresponding to 20 MTs) were scrutinized and 76 new bindings were counted (Fig. 2 B). The result revealed a biased distribution in the plus-end direction; within a 6- μm distance, binding in the plus-end direction was 2.2 times higher than the binding in the minus-end direction (52 plus-end events vs. 24 minus-end events). Assuming no particular preference in the direction of cooperative binding, the probability of such an uneven distribution within statistical fluctuation is $< 0.2\%$ (chi-square test).

Directional, cooperative binding was also confirmed in another experiment where a kinesin bead was first fixed on the MT and then the subsequent binding of other kinesin beads was examined (Fig. 3 A). This experiment was designed to more efficiently analyze the directionality of cooperative binding. To make a kinesin bead stationary on the MT in the presence of ATP, we used a previously constructed heterodimeric kinesin, WT/E236A, which can hydrolyze ATP, and yet remain fixed on the MT (Table S1, available at <http://www.jcb.org/cgi/content/full/jcb.200409035/DC1>; Kaseda et al., 2002). In addition to this refinement, compared with the previous experiment shown in Figs. 1 and 2, we lowered both the kinesin density on the beads and the concentration of beads used in the binding assay, thereby increasing the chance of lone bindings (see Materials and methods for details).

Before the binding assay, fluorescent latex beads with a diameter of 0.5 μm were first coated with WT/E236A via a streptavidin–biotin interaction, and these WT/E236A-beads were bound to MTs in the absence of ATP (Fig. 3 A, Step 1, fixing a reference bead to an MT). Subsequently, binding of other kinesin beads (0.2 μm in diameter, coated with wild-type kinesin) to these MTs was tested in the presence of ATP (Fig. 3 A, Step 2, binding assay using test beads). To guarantee equal opportunity for binding in either direction, again, only those MTs with a single reference bead bound and having $> 6 \mu\text{m}$ of free MT on either side of the reference bead were analyzed. A homodimer of E236A showing no ATPase activity (Table S1) was used as a control to coat the reference bead.

First, to validate the usage of WT/E236A, we measured the distribution of binding frequency along the MTs with a

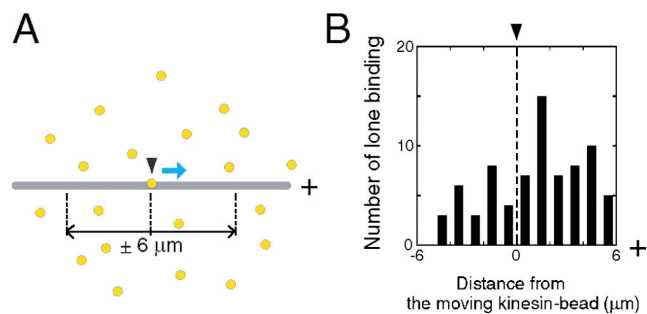


Figure 2. **Directional preference of cooperative binding.** (A) Schematic representation of the analysis of lone binding. (B) Distribution of the lone binding summed for 20 MTs. In both A and B, an arrowhead indicates the position of the preexisting, moving kinesin bead. As multiple kinesin beads were simultaneously moving along the MT most of the time, only 2% of the total binding events was counted for this lone-binding analysis.

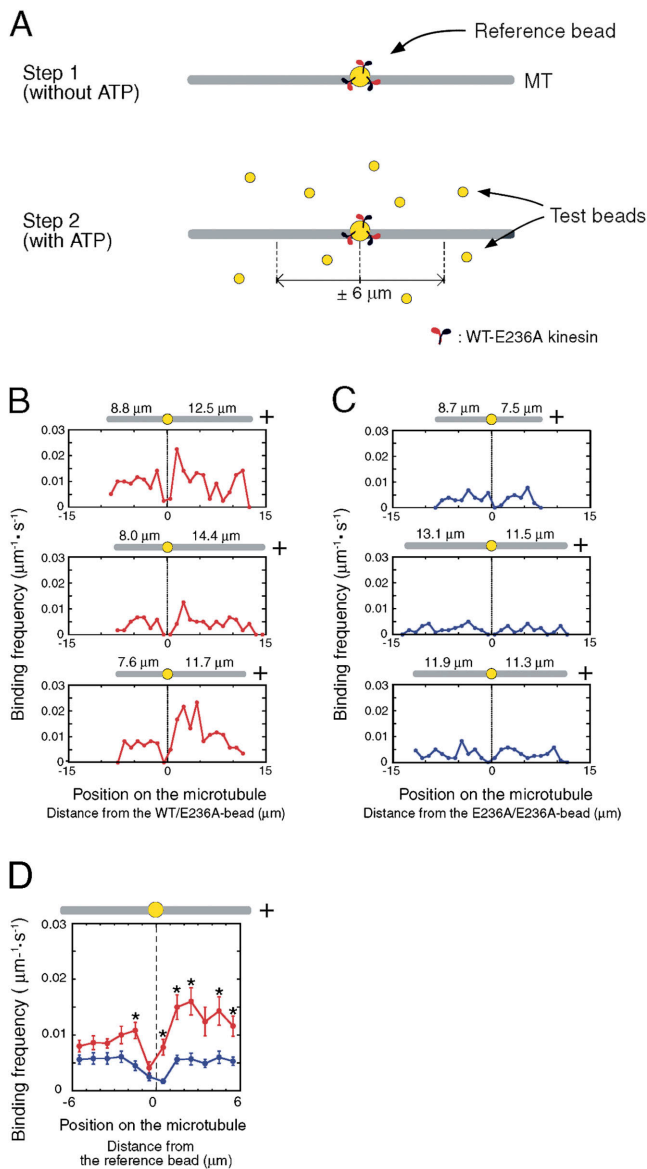


Figure 3. Cooperative binding induced by heterodimeric kinesin, WT/E236A. (A) Schematic representation of binding assay using heterodimeric kinesin. (B) Three representative example distributions of binding frequency for a MT with a bound WT/E236A-bead. Total binding number and observation time is (from top to bottom) 324, 1,174 s; 158, 1,200 s; 292, 1,193 s. (Video 2). (C) Three example distributions for a MT with a bound E236A/E236A-bead. Total binding number and observation time is (from top to bottom) 99, 1,026 s; 78, 1,200 s; 119, 1,200 s. In both B and C, binding was suppressed in the immediate vicinity of the reference bead due to physical obstruction of the binding site by the reference bead. Length of the MT on either side of the reference bead, measured from the center of the bead, is indicated in the graph. Bin size = 1 μm . (D) Distribution of the binding frequency averaged for 10 MTs within a 6- μm distance either side of the reference bead. The red line is for MTs with a bound WT/E236A-bead (1,429 bindings were counted over a total observation period of 187 min) and the blue line is for MTs with a bound E236A/E236A-bead (699 bindings were counted over a total observation period of 196 min). Asterisks indicate that the difference in mean binding frequencies between the two groups was significant ($P < 0.01$; t test). Error bar indicates SEM. Bin size = 1 μm . Note that the absolute value of the binding frequency in this experiment cannot be directly compared with the binding frequency shown in Fig. 1 C, because the conditions of the wild-type-kinesin beads were different between the two experiments (see Materials and methods).

bound WT/E236A-bead. The result showed that binding of the test beads was enhanced in the vicinity of the WT/E236A-bead, most prominently in the plus-end direction (Fig. 3 B, Video 2, available at <http://www.jcb.org/cgi/content/full/jcb.200409035/DC1>). The degree of enhancement varied between experiments. In contrast, for MTs with a bound E236A/E236A-bead, the binding frequency was low and no significant bias was detected (Fig. 3 C). When the binding frequency averaged for 10 MTs was compared between the two groups, the frequency was significantly higher for MTs with a WT/E236A-bead (Fig. 3 D). These results are consistent with the result shown in Fig. 1 C, which indicated ATP hydrolysis is essential for cooperative binding.

Now to evaluate the directionality of cooperative binding, based on the same binding data, only those new bindings occurring in the absence of any other beads moving on the MT were counted. Although the experimental conditions were optimized here to increase the chance of lone bindings occurring, the value for total bindings shown in Fig. 3 B may still include those bindings that are facilitated by the presence of other test beads on the MT (Fig. 4 A). The distribution of the lone bindings revealed that for MTs with a bound WT/E236A-bead, the binding was significantly higher in the plus-end than the minus-end direction (205 plus-end events and 115 minus-end events, $P < 0.01$; chi-square test; Fig. 4 B). In contrast, for MTs with a bound E236A/E236A-bead, distribution of lone bindings was not significantly biased (203 plus-end and 211 minus-end events, $P = 0.694$; chi-square test; Fig. 4 C). We conclude that cooperative binding induced genuinely by the WT/E236A-bead was biased toward the plus-end direction.

In an independent series of experiments, the directionality of lone binding was also examined in the presence of either ADP or AMP-PNP for MTs with a bound WT/E236A-bead. In both conditions, no significant directional bias was detected (for ADP, 57 plus-end and 59 minus-end events, $P = 0.853$; for AMP-PNP, 56 plus-end and 53 minus-end events, $P = 0.774$; chi-square test).

Together, the results show that binding of kinesin beads to a MT is cooperative in the presence of ATP and that it is biased toward the MT plus end. It is unlikely that cooperative binding over micrometers in MT length is the result of electrostatic attraction between kinesin beads (Israelachvili, 1985). Rather, the results can be explained if MTs have more than two binding-affinity states for kinesin beads. Under this model, in the presence of ADP or AMP-PNP, MTs remain in a low affinity state along their entire length, while in the presence of ATP, binding of a kinesin bead to a MT might induce transition of the MT to a state with higher affinity for other kinesin beads over a range of micrometers. As the E236A/E236A-bead was unable to induce cooperative binding, ATP hydrolysis by kinesin is essential for inducing the state transition in the MT.

What then is the role of state transition in MTs? One possibility is in the regulation of motility. In lobster axons, quantitative analysis of the number of vesicles associated with individual MT revealed that MTs in axons exist in two populations, each having a different affinity for vesicles (Miller et al., 1987). In vivo, organelle transport could be regulated by alter-

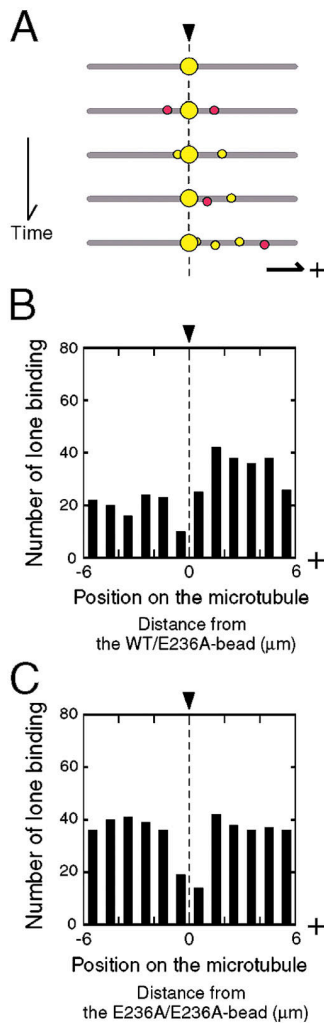


Figure 4. Directionality of lone binding. (A) Schematic illustration of a representative sequence of binding events. Arrowhead indicates the position of the WT/E236A-bead. New bindings are colored red and turn yellow in subsequent images. Total binding counted in Fig. 3 B may include those that are genuinely induced by the WT/E236A-bead and those that are facilitated by the presence of other test beads. Even if the cooperative binding induced genuinely by the WT/E236A-bead was symmetric, the movements of these bound beads toward the MT plus end might lead to the asymmetric distribution of the subsequent binding. (B) Distribution of the lone bindings summed for 10 MTs with a bound WT/E236A-bead (total 320 bindings). (C) Distribution of the lone bindings summed for 10 MTs with a bound E236A/E236A-bead (total 414 bindings). In both B and C, bin width is 1 μm . With a similar observation time (~ 190 min), more lone bindings were counted for MTs with a bound E236A/E236A-bead as compared with the MTs with a bound WT/E236A-bead. This result is not surprising given that less frequent binding means a larger fraction of lone bindings in the total binding count.

ation of the MT affinity states. Furthermore, our result that the cooperative binding was biased in the plus-end direction suggests a possibility that anisotropy in the potential of kinesin–MT interaction might contribute to the directional movement of kinesin (Okada and Hirokawa, 1999).

Structural studies of MTs and tubulin sheets have revealed that the binding of kinesin in the presence of AMP-PNP induces a conformational change in tubulin dimers (Hoenger and Milligan, 1997; Krebs et al., 2004). It is of interest to know

how the structure of the kinesin–MT complex changes during ATP hydrolysis. Because the movement of motors should involve an intimate and concerted partnership between the motor and the cytoskeletal filaments, understanding the role of cytoskeletal filaments could be essential to the complete elucidation of the motility mechanism.

Materials and methods

Binding assay under various nucleotide conditions

Tubulin and kinesin were purified from bovine brain as outlined by Kojima et al. (1997). Tetramethylrhodamine-labeled MTs were prepared as described previously (Miyamoto et al., 2000). To prepare kinesin-coated beads, fluorescent latex beads (carboxylate modified, 0.2 μm in diameter, 10% wt/vol; F-8811; Molecular Probes) were first incubated with an equal volume of casein solution (5 mg/ml in 10 mM Tris, 0.1 M NaCl) for 30 min on ice. The bead–casein mixture was subsequently combined with a 0.63 μM kinesin solution and 1 M NaCl at a volume ratio of 2:1:0.3, and incubated for 4 h on ice. Using this protocol, virtually all the kinesin molecules in solution were adsorbed on the surface of the latex beads (determined by folin; Lowry et al., 1951), and thus the molar stoichiometry of kinesin to bead was estimated to be 17 molecules per bead.

For binding assays in the presence of ATP, MTs (10 $\mu\text{g}/\text{ml}$) in buffer A (20 mM Pipes, 10 mM K-acetate, pH 6.8, 4 mM MgSO_4 , 2 mM EGTA, 0.2 mM EDTA) supplemented with 10 μM taxol (T-7402; Sigma-Aldrich) were introduced to a flow chamber made of two coverslips (dimensions 10 mm \times 10 mm \times 110 μm). The bottom coverslip was pretreated with Sigmacote (SL2; Sigma-Aldrich) and the MTs tended to stick to its surface for their entire length. In the following procedure, 10 μM taxol was always included. After a 3-min incubation with the MT solution, 20 μl of casein solution was introduced to the chamber. After another 5-min incubation, the chamber was extensively washed with 40 μl of buffer A and loaded with 20 μl of kinesin-bead solution (kinesin-coated beads prepared as above and diluted to a concentration of 90 pM in buffer A including 1 mM ATP and an oxygen scavenger [Miyamoto et al., 2000]). The flow chamber was sealed with vaseline and observed under an inverted fluorescence microscope (TMD-300; Nikon) equipped with an oil immersion objective lens (Neofluar, 100 \times , NA = 1.3; Carl Zeiss Micro-Imaging, Inc.) and a SIT camera (C2400-8; Hamamatsu Photonics). The observation was made at $26 \pm 1^\circ\text{C}$ and the image was recorded using a digital video recorder (DSR20; Sony).

For binding assays in the presence of ADP or AMP-PNP, as kinesin beads are difficult to dissociate once bound to MTs in these nucleotide conditions, the number of kinesin beads on the MT increased with time. To observe this process from the start, MTs were first allowed to attach to the bottom of the flow chamber, and then viewed under a fluorescence microscope. The kinesin-bead solution including 1 mM ADP or AMP-PNP was subsequently introduced to the chamber so that the process of their binding to the MTs could be monitored in real time by fluorescence microscopy. Images of the binding were recorded until the average bead density on the MT approached 0.58 beads/ μm , which was the maximum bead density achieved in the experiment in the presence of ATP. In the case of AMP-PNP, the solution was supplemented with apyrase (A-6132, 1 U/ml; Sigma-Aldrich).

Analysis of cooperativity

Statistical significance of cooperativity was examined by comparing the PDD expected for random binding and the PDD of actual binding by the Kolmogorov-Smirnov test (Fig. S1). If the binding was random along the MTs, N should be a linear function of L in each window. Then, the PDD of actual binding,

$$N_i / \sum_{i=2}^9 N_i,$$

is expected to coincide with the PDD of the MT length,

$$L_i / \sum_{i=2}^9 L_i,$$

where N_i and L_i are the total number of bindings and the total length of MT in the i th window from the preexisting kinesin bead, respectively. The window closest to the preexisting kinesin bead ($i = 1$) was omitted from

the calculation, because in this area, binding was suppressed due to physical obstruction of the binding site.

Preparation of kinesin constructs and ATPase assays

The homodimeric and heterodimeric E236A mutants were prepared as described previously (Kaseda et al., 2002). Steady-state MT-activated ATPase was measured using malachite green (Kodama et al., 1986).

Binding assay using MTs with a bound WT/E236A- or E236A/E236A-bead

To make the WT/E236A- and E236A/E236A-beads, carboxylated fluorescent latex beads with a diameter of 0.5 μm (L-5261; Molecular Probes) were coated with streptavidin and subsequently incubated with WT/E236A or E236A/E236A as described previously (Kaseda et al., 2003). Labeling stoichiometry of the reference beads, estimated from their probability of movement in optical nanometry (Kojima et al., 1997), was ~ 100 homodimers and ~ 25 heterodimers to a bead on average.

To prepare test beads for the binding assay, 0.2- μm diam fluorescent latex beads were coated with native kinesin as described previously (Binding assay under various nucleotide conditions), except that the stoichiometry of kinesin to a bead was 12 and the final concentration of the beads used in the binding assay was 80 pM.

For the binding assay, MTs were made attached to the bottom of the flow chamber and 20 μl of casein solution including 10 μM taxol was introduced to the chamber, and incubated for 10 min. In the following procedure, 10 μM taxol was always included. The chamber was washed with 30 μl of buffer A and then loaded with 20 μl of WT/E236A- or E236A/E236A-bead solution (3 pM). After an 8-min incubation, the chamber was extensively washed with 60 μl of buffer A to remove the beads not bound to MTs. Finally, 15 μl of test-bead solution including 1 mM ATP and an oxygen scavenger was introduced into the chamber, and the binding was observed under fluorescence microscope. MTs with only one reference bead attached and having $> 6 \mu\text{m}$ of MT length on either side of the reference bead were imaged for 20 min.

For binding assays in the presence of ADP or AMP-PNP for MTs with a bound WT/E236A-bead, the protocol was same as above except that the nucleotide included in the final test-bead solution was 1 mM ADP or AMP-PNP. Because the test beads only showed minimal dissociation from the MTs in the presence of these nucleotides, we counted only one lone binding from a single MT. In each experiment, after the observation of the initial binding event, test-bead solution including 1 mM ATP was freshly introduced into the chamber and the polarity of this single MT was determined by the direction of the movement of the beads.

Online supplemental material

Online supplemental material includes: Fig. S1 showing statistical analysis of kinesin-bead binding; Table S1 showing kinetic and motile properties of heterodimeric and homodimeric E236A kinesin; and Videos 1 and 2, corresponding to data in Figs. 1 A and 2 B, respectively. Online supplemental material is available at <http://www.jcb.org/cgi/content/full/jcb.200409035/DC1>.

We thank T. Yanagida, M. Tokunaga and S. Usui for their valuable comments. The authors also thank Y. Miyamoto for help in writing the statistical analysis program, and S. Ishiwata, S. Kamimura, S. Matsuura, N. Murphy, M. Nishiyama, F. Oosawa, G.H. Pollack, and R.D. Vale for critical reading of the manuscript.

Submitted: 7 September 2004

Accepted: 20 January 2005

References

Block, S.M., L.S. Goldstein, and B.J. Schnapp. 1990. Bead movement by single kinesin molecules studied with optical tweezers. *Nature*. 348:348–352.

Burlacu, S., and J. Borejdo. 1992. Motion of actin filaments in the presence of myosin heads and ATP. *Biophys. J.* 63:1471–1482.

Crevel, I.M., A. Lockhart, and R.A. Cross. 1996. Weak and strong states of kinesin and ncd. *J. Mol. Biol.* 257:66–76.

Hackney, D.D. 1994. Evidence for alternating head catalysis by kinesin during microtubule-stimulated ATP hydrolysis. *Proc. Natl. Acad. Sci. USA*. 91:6865–6869.

Hoenger, A., and R.A. Milligan. 1997. Motor domains of kinesin and ncd interact with microtubule protofilaments with the same binding geometry. *J. Mol. Biol.* 265:553–564.

Howard, J. 1996. The movement of kinesin along microtubules. *Annu. Rev.*

Physiol. 58:703–729.

Howard, J., A.J. Hudspeth, and R.D. Vale. 1989. Movement of microtubules by single kinesin molecules. *Nature*. 342:154–158.

Israelachvili, J.N. 1985. Intermolecular and Surface Forces. Academic Press, New York. Chapter 12. 450 pp.

Kaseda, K., H. Higuchi, and K. Hirose. 2002. Coordination of kinesin's two heads studied with mutant heterodimers. *Proc. Natl. Acad. Sci. USA*. 99:16058–16063.

Kaseda, K., H. Higuchi, and K. Hirose. 2003. Alternate fast and slow stepping of a heterodimeric kinesin molecule. *Nat. Cell Biol.* 5:1079–1082.

Kim, E., E. Bobkova, C.J. Miller, A. Orlova, G. Hegyi, E.H. Egelman, A. Muhlrad, and E. Reisler. 1998. Intrastrand cross-linked actin between Gln-41 and Cys-374. III. Inhibition of motion and force generation with myosin. *Biochemistry*. 37:17801–17809.

Kodama, T., K. Fukui, and K. Kometani. 1986. The initial phosphate burst in ATP hydrolysis by myosin and subfragment-1 as studied by a modified malachite green method for determination of inorganic phosphate. *J. Biochem. (Tokyo)*. 99:1465–1472.

Kojima, H., E. Muto, H. Higuchi, and T. Yanagida. 1997. Mechanics of single kinesin molecules measured by optical trapping nanometry. *Biophys. J.* 73:2012–2022.

Krebs, A., K.N. Goldie, and A. Hoenger. 2004. Complex formation with kinesin motor domains affects the structure of microtubules. *J. Mol. Biol.* 335:139–153.

Lowry, O.H., N.J. Rosebrough, A.L. Farr, and R.J. Randall. 1951. Protein measurement with the folin phenol reagent. *J. Biol. Chem.* 193:265–275.

Miller, R.H., R.J. Lasek, and M.J. Katz. 1987. Preferred microtubules for vesicle transport in lobster axons. *Science*. 235:220–222.

Miyamoto, Y., E. Muto, T. Mashimo, A.H. Iwane, I. Yoshiya, and T. Yanagida. 2000. Direct inhibition of microtubule-based kinesin motility by local anesthetics. *Biophys. J.* 78:940–949.

Okada, Y., and N. Hirokawa. 1999. A processive single-headed motor: kinesin superfamily protein KIF1A. *Science*. 283:1152–1157.

Rice, S., A.W. Lin, D. Safer, C.L. Hart, N. Naber, B.O. Carragher, S.M. Cain, E. Pechatnikova, E.M. Wilson-Kubalek, M. Whittaker, et al. 1999. A structural change in the kinesin motor protein that drives motility. *Nature*. 402:778–784.

Schnapp, B.J., B. Crise, M.P. Sheetz, T.S. Reese, and S. Khan. 1990. Delayed start-up of kinesin-driven microtubule gliding following inhibition by adenosine 5'-[beta, gamma-imido]triphosphate. *Proc. Natl. Acad. Sci. USA*. 87:10053–10057.

Vilfan, A., E. Frey, F. Schwabl, M. Thormahlen, Y.H. Song, and E. Mandelkow. 2001. Dynamics and cooperativity of microtubule decoration by the motor protein kinesin. *J. Mol. Biol.* 312:1011–1026.

Yanagida, T., M. Nakase, K. Nishiyama, and F. Oosawa. 1984. Direct observation of motion of single F-actin filaments in the presence of myosin. *Nature*. 307:58–60.